

THE IMPACT OF USING DIFFERENT FUEL DENSITIES ON THE NEUTRONIC PARAMETERS OF MATERIAL TEST RESEARCH (MTR) REACTOR CORE

Rani O.A. Aziz^a, E. H. Amin^b, W. M. Seif^a, H. Abou-Shady^{a,*}

^a Physics Department-Faculty of Science, Cairo University, Giza, Egypt

^b National Center of Nuclear Safety and Radiation Control, Atomic Energy Authority, Cairo, Egypt

Abstract: The deterministic neutronic analysis approach is used to study the effect of varying fuel densities on the neutronic parameters of Material Test Research reactors core. The core configuration is that of the first equilibrium core of Pakistan Research Reactor-1 (PARR-1). Fuel elements with uranium densities 3.2, 3.28, 3.6, 3.8, 4, 6, 8, 10 and 15 g/cm³ are proposed instead of the existing fuel elements. The proposed fuel densities are used to operate the cores with the same characteristics of the first equilibrium core of PARR-1 reactor for a power of 9 MW and cycle length of 40 effective full powerdays. The impact of fuel density change on the core reactivity, multiplication factor, flux, power density and burnup distribution are studied. By increasing the fuel density to 25, 50 and 150% the core reactivity has increased by 60, 50 and 25% respectively. No significant impact of using fuel densities greater than 6 g/cm³ was found with the existing core configuration and operating characteristics. The thermal neutron flux in the central flux trap decreased by 19.2% with the fuel density increase to 6 g/cm³ and decreased by 34.6% with the fuel density increase to 15 g/cm³. At the end of cycle, the power density distribution decreased with the increase of the fuel density for all fuel elements except that those around the central flux trap. The theoretically calculated cycle length for cores using fuel elements with the densities 3.6, 3.8, 4.0 and 6.0 g/cm³ were found to be 43.9, 46.3, 48.8 and 73.2 days respectively.

Keywords Research reactors - MTR fuel density - Neutronic analysis - MTR reactor core design

* Corresponding author. Tel.: +202 01223259615.

E-mail address: hodamfas@hotmail.com , hoda@sci.cu.edu.eg (H. Abou-Shady).

1. Introduction:

A large number of research reactors are used for different purposes. High flux research reactors play a significant role in providing facilities for basic research in various areas of science and applied research related to the development and testing of nuclear fuels and numerous materials. Most of the research reactors around the world that use highly enriched uranium (HEU) fuel are being shutdown or converted to low enriched uranium (LEU) fuel due to proliferation concerns [1,2]. The advantage of using HEU fuel are higher power densities that results in higher neutron flux, higher fuel burnup, longer fuel cycle and smaller radioactive waste [3]. The reduced fuel enrichment decreases the amount of fissile material resulting in a reduced core life. To overcome this situation, higher loading of LEU fuel required to compensate for increased absorption of neutrons in U-238 resonance peaks. Consequently, the core volume was increased and neutron fluxes for irradiation and isotope production were decreased. By increasing the power of the converted core, the neutron fluxes in the core and at irradiation sites can be increased. The power up gradation depends on the capability of thermal hydraulic system. However, if the low density HEU fuel is replaced with high-density LEU fuel, the core may offer fluxes of similar magnitude as offered in HEU core. Thus, high density uranium fuels are being developed [4].

In general, any increase in fuel uranium density increases the excess reactivity, hardens the neutron flux spectrum, decreases the prompt neutron generation time and effective delayed neutron fraction, increases the Doppler reactivity feedback coefficient and decreases the coolant temperature and density feedback coefficients. Any change in the enrichment or the density changes the core neutronics and thermal hydraulics of the reactor and as a result transient response of the reactor is also affected. Therefore, detailed neutronics and thermal hydraulics calculations are required to assess the core safety under normal and accidental operating conditions [1, 2, 5, and 6].

The validation of the Standard computer codes WIMS-D and CITATION to study the criticality [7] and reactor physics calculations [8] of a typical swimming pool type material test research reactor had been published.

Because research reactors are mainly used for the production of neutrons, the utilization capacity of research reactors in terms of radioisotopes production, material test, neutron transmutation, and neutron diffraction is directly related to the magnitude of the neutron flux in the irradiation positions. Hence optimization of the neutron fluxes in the experimental channels and irradiation positions is of great importance in research reactor utilization. In the present paper, the impact of fuel density change on three essential core parameters; the neutron fluxes in the in-core irradiation position, the burnup distribution and the power density distribution has been studied.

2. Description of the Reactor Core Configuration:

The reactor core selected is the first equilibrium core of the Pakistan Research Reactor-1 (PARR-1), operated by Pakistan Institute of Nuclear Science and Technology (PINSTECH). It is a general purpose MTR type swimming pool type research reactor. Converted in 1991 from 93% high enriched uranium (HEU) fuel to 19.99% low enriched uranium (LEU) fuel in the form of U_3Si_2-Al . During the conversion program its power was upgraded from 5 MW to 9 MW then to 10 MW. The core configuration used in the present work is shown in Fig. 1. It consists of standard and control fuel elements mounted on a grid plate to assemble the core. The core is immersed in demineralized light water that acts as coolant, moderator, and reflector. However, using specially designed reflector elements. Light water could be replaced by other reflector materials such as graphite or beryllium [9]. The design data description is tabulated in Table 1 [10].

A 2D view for the Standard fuel element (SFE) is shown in Fig. 2 [11]. In standard fuel elements, there are 23 plates per fuel element and ^{235}U loading per fuel element is 290g. All the plates are fuel bearing and there are no dummy plates and the outer two plates have higher clad thickness, i.e. 0.495 mm. The physical dimensions of the fuel are such that there is a water gap of 1.19 mm between the side plates of two adjacent fuel elements. Similarly there is a water gap of 1.37mm between two fuel elements in the direction perpendicular to the fuel plates. The coolant channel width is 2.1 mm [9].

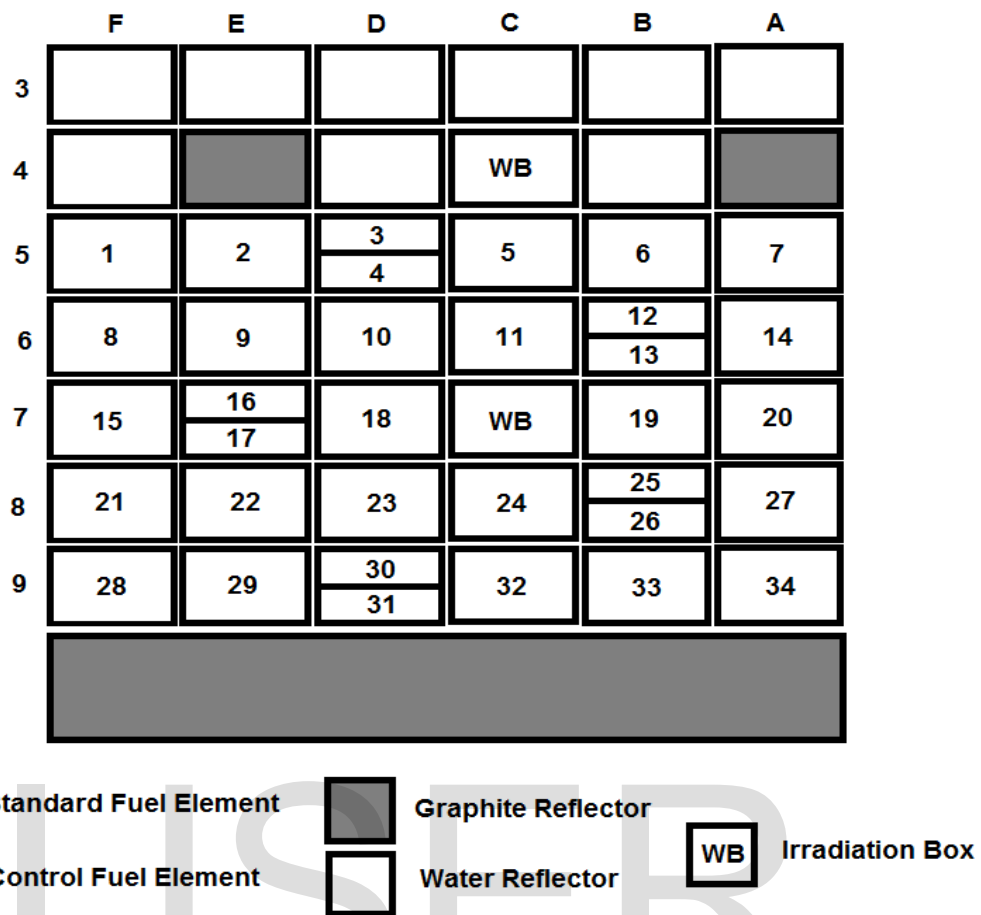


Figure 1: First equilibrium core configuration.

The control fuel element (CFE) 2D cross-sectional view shown in Fig. 3 [11]. There exists an empty space in the center of the fuel regions, i.e. a control gap (including guide plates and extra cooling channels) sandwiched between fuel bearing regions. The fuel plates are identical to those in the standard fuel element. In the control region, the thickness of the side plates is 0.7085 cm. each control fuel element has 13 fuel plates and 235U loading per control fuel element is 164 g. The overall physical dimensions of CFE are the same as that of the SFE [9].

Table 1: Design Parameters of Pakistan Research Reactor-1[10]

Reactor type	Pool type MTR
Steady state power level (MWth)	9
Grid plate	9 X 6
Lattice pitch (mm)	81.0-77.11
Fuel material	U3Si2-Al
Fuel enrichment (% by wt)	19.99
Cladding material	Al
Coolant	H2O
Moderator	H2O
Refractory	H2O+graphite
Fuel element dimensions (mm)	79.63-75.92
Number of fuel plates in (SFE/CFE):	(23/13)
Shape of fuel plates	Flat
Total width of plates (mm)	66.92
Total length of fuel plate (mm)	625.00
Thickness of fuel plates (mm)	
Inner plates	1.27
Outer plates	1.50
Thickness of clad (mm)	
Inner plates	0.380
Outer plates	0.495
Thickness of side plates (mm)	4.500
Length of side plates (mm)	724.000
Fuel meat dimensions (mm)	
Length	600.00
Width	62.75
Thickness	0.51
Water channel thickness (mm)	2.10
Water gap between side plates of two fuel elements (mm)	1.19

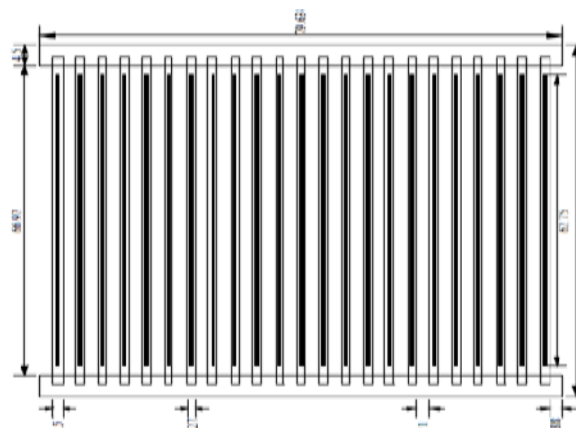


Figure 2: 2D view for the standard fuel element [11].

energy and directional subdivisions. Specialized deterministic computer codes solve these coupled linear algebra equations for the neutron flux in each phase cell, and the desired flux integrals are approximated by summations over the appropriate cells to get the engineering parameters (including k-effective) of interest in the analysis.

Mathematical methods are used in solving the neutron diffusion equation with some approximations. The finite difference form of the neutron diffusion equation is the one that used by our code CITVAP. In Eq. 1 the diffusion approximation to neutron transport at some location r and energy E in a finite difference type of neutron balance over discrete elements of volume are tabulated [14]:

$$-\nabla D_{r,E} \nabla \Phi_{r,E} + (\Sigma_{a,r,E} + \Sigma_{s,r,E}) \Phi_{r,E} = \int_{E'} \left(\Sigma_{r,E' \rightarrow E} + \frac{\chi_E (v\Sigma)_{f,r,E'}}{K_e} \right) \Phi_{r,E'} dE' \text{ ----- (1)}$$

In **Eq. 2** the continuous energy spectrum is divided into discrete energy groups, a buckling term is allowed when appropriate, the source distribution function, χ , is assumed to have no spatial dependence, and a simplification is made in the transport term [14]:

$$-D_{r,g} \nabla^2 \Phi_{r,g} + \left(\Sigma_{a,r,g} + \sum_n \Sigma_{s,r,g \rightarrow n} + D_{r,g} B_{1g}^2 \right) \Phi_{r,g} = \sum_n \left(\Sigma_{s,r,n \rightarrow g} + \frac{\chi_g (v\Sigma)_{f,r,n}}{K_e} \right) \Phi_{r,n} \text{ ---(2)}$$

Where:

$\nabla^2 \equiv$ Laplacian operator

$\Phi_{r,g} \equiv$ neutron flux at location r and for energy group g

$\Sigma_{a,r,E} \equiv$ Microscopic absorption cross section

$\Sigma_{s,r,g \rightarrow n} \equiv$ Macroscopic scattering cross section from group g

$D_{r,g} \equiv$ Diffusion cross section for energy group g

$\chi_g \equiv$ Function for source neutron

$(v\Sigma)_{f,r,n} \equiv$ Macroscopic production cross section

$K_e \equiv$ effective multiplication factor

$B_{1g}^2 \equiv$ Buckling term

Because the basic formation of the deterministic solution requires this extensive subdivision, deterministic methods naturally provide the detailed information in space and energy that the reactor design process requires. In addition to this wide range of information that they deliver, the deterministic methods also tend to be fast, accurate, and amenable to acceleration and convergence improvement methods from well-developed numerical analysis techniques [15]. In the present work the deterministic method used for reactor core analysis. The CITVAP code used for whole core to calculate the effective multiplication factor and the reactivity of the reactor beside other core parameters like fluxes distribution, power distribution, and burnup distribution by simulating the core in x-y-z geometry. All control rods are fully withdrawn. The CITVAP code needs the group constants (macroscopic absorption cross section, the nu-fission cross section, the diffusion coefficient, the scattering matrix, and the fission spectrum for all neutron energy groups) for the different regions in the core as input data. For the generation of the group constants for the different regions in the core, WIMSD code used, It was necessary to model each region of the core separately to obtain the cross sections for the different regions of the core, i.e. standard fuel element, control fuel element, irradiation boxes, and water and graphite reflectors.

3.2 Cores with different densities:

Different cores using fuel elements with densities 3.2, 3.28, 3.6, 3.8, 4, 6, 8, 10 and 15 g/cm³ were considered. All cores are in the same configuration as that for the first equilibrium core of PARR-1, which contains 29 standard fuel elements and 5 control fuel elements beside two in-core irradiation positions, one is the central flux trap in the middle of the core and the other in the side of graphite reflector. The operating characteristics of all the cores are the same. They are operated with a power of 9MW for 40 effective full power days (EFPD) cycle length.

4. Results and Discussion:

4.1 Fresh cycle:

The burnup percentage is shown in Fig. 4 as a function of time for the standard fuel element with the proposed densities. This will be used later as a guide to estimate the suitable cycle length for each density. The reference density is 3.28 g/cm^3 at which the cycle length is 40 EFPD and the equilibrium cycle is achieved after 5 cycle. The equilibrium cycle is defined as the cycle whose parameters do not change from one cycle to the subsequent cycle [16] which means that the fuel element will be in the core for approximately 200 to 240 EFPD. The standard fuel element was burned for 300 days to ensure that all expected times will be counted in the burnup. A linear fitting for each density was performed to deduce the cycle length at which the reference burnup criteria are met. The above strategy is suggested for estimating the cycle length at the beginning. For the same power level, the specific power changed with the fuel density as shown in table below. This specific power is used to follow the change in the amount of fuel element irradiation after 240 FPD cycle. The irradiation after 240 effective full power days (EFPD) calculated theoretically for each fuel density are tabulated in Table 2. The estimated time required to reach the same level of fuel irradiation as that for fuel with density 3.28 g/cm^3 after 240 (EFPD), are shown in Table 3.

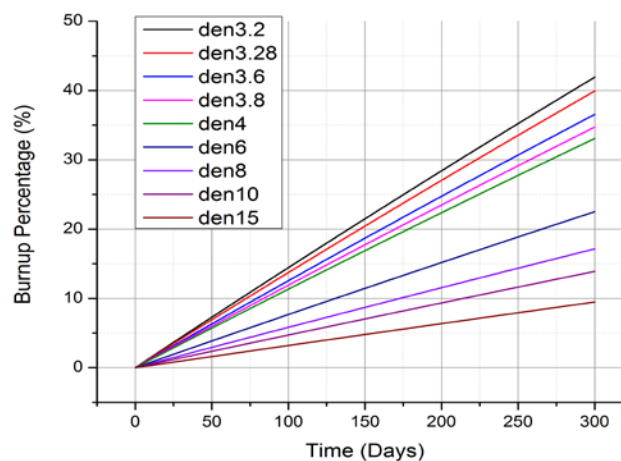


Figure 4: Burnup percentage as a function of time for different fuel uranium density.

Table 2: Irradiation after 240 EFPD.

Density (g/cm ³)	Specific Power (MW/Te)	Irradiation after 240 FPD (MWD/Te)
3.2	231.23	55495.2
3.28	219.613	52707.12
3.6	200.09	48021.6
3.8	189.56	45494.4
4	180.83	43399.2
6	120.055	28813.2
8	90.041	21609.84
10	72.033	17287.92
15	48.022	11525.28

Table 3: Estimated time required to reach irradiation of 52707.12 MWD/Te.

Density (g/cm ³)	Time required to reach irradiation 52707.12 MWD/Te	Time required/6 The expected cycle length
3.28 reference	240 FPD	40
3.6	263.4	43.9
3.8	278.05	46.3
4	292.69	48.78
6	439.04	73.17
8	585.37	97.56
10	731.71	121.95
15	1097.56	182.92

A comparison of the multiplication factor (k_{eff}) during one operating cycle with a length of 40 EFPD for each fuel density proposed provides in Fig. 5. The multiplication factor describes the average and global behaviour of the core (R. Khan Austria-prnt-flash). As can be seen from the figure, by using the existing core configuration with out any modifications the change in k_{eff} during one operating cycle are depend on the fuel density used. The k_{eff} is changed between the begine of cycle (BOC) and the end of cycle (EOC) for the different densities proposed 3.2, 3.28, 4, 8 and 15 g/cm³ by an amount of 3.2, 2.8, 2.0, 1.7 and 0.8% respectively. Also Fig. 5 shows the impact of fuel density change on the multiplication fctor of the core. It present values at each five days. It shows that by increasing the fuel density from 3.2 to 4 the k_{eff} is increased from 1.09 to 1.11 at BOC and from 1.05 to 1.09 at EOC, means that 25% change in the density will be followd by 1.8% change in the K_{eff} at BOC and 3.8% at EOC. By increasing the density from 3.2 to 6 (87.5% density change) the k_{eff} is increased by 5.5% at BOC and 7.6% at EOC. By increasing the density

from 3.2 to 8 g/cm³ (150% density change) the k_{eff} is increased by 7.3% at BOC and 9.5% at EOC. By increasing the density from 3.2 to 15 g/cm³ (369% density change) the k_{eff} is increased by 9.2% at BOC and 12.4% at EOC.

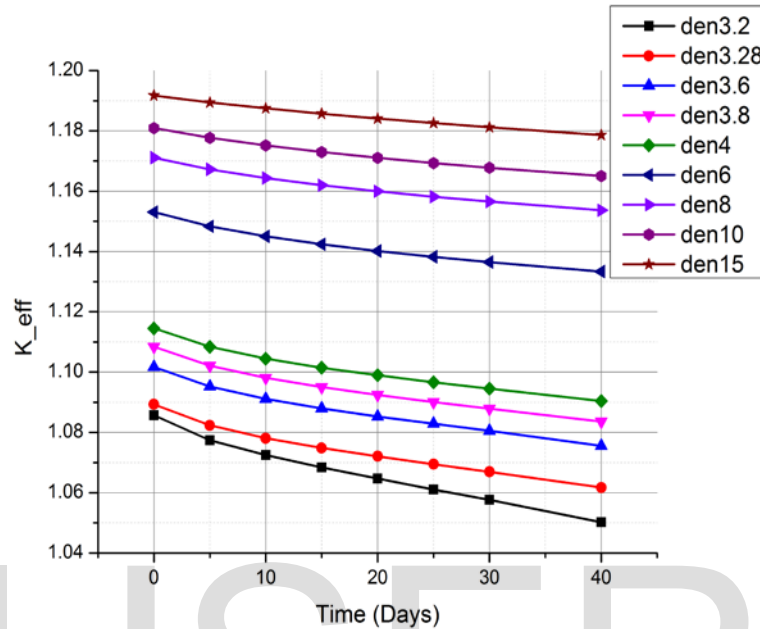


Figure 5: Core Multiplication factor as a function of time for different fuel densities.

The change in reactivity as a function of density presents in Fig. 6. It shows values at the beginning and at the end of operation cycle with a length of 40 effective full power day (EFPD). Three regions of density impact on reactivity can be seen in the figure. The first region with a very sharp change begin from density 3.2 g/cm³ with 5000 pcm to density 4 g/cm³ with 8000 pcm (25% density increase followed with impact of 60% reactivity increase). The second region begin from density 4 to 6 g/cm³ (50% density increase followed with impact of 50% reactivity increase). The third region begin from density 6 to 15 g/cm³ (150% density increase followed with impact 25% reactivity increase). From the results shown in the Fig. 3 it can be seen that by increasing the density above 6 g/cm³ with using the same core configuration of the first equilibrium core and with the same operating characteristics of that core there is no very sharp impact on the reactivity.

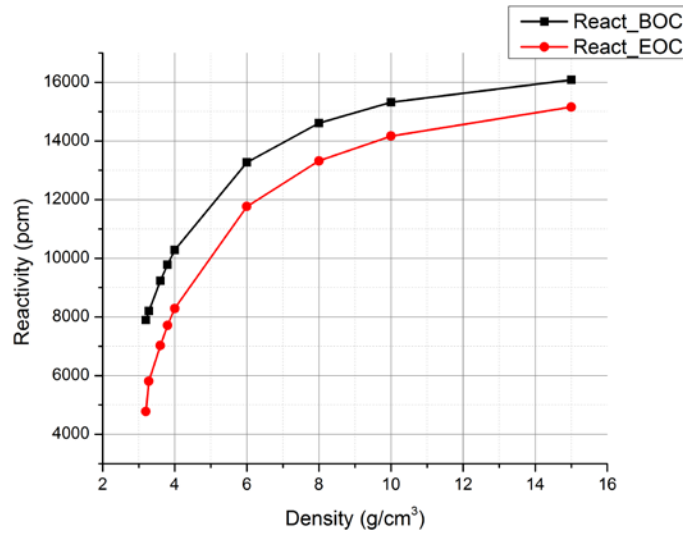


Figure 6: Core reactivity as a function of fuel uranium density.

The plot of fluxes in the central irradiation position as a function of density change are shown in Fig. 7. As can be seen from the figure the thermal neutrons flux has the maximum impact of density change. By increasing the density from 3.2 to 6 g/cm³ the thermal neutron decreased by 19.2%, while by increasing the density to 15 g/cm³ the thermal flux decreased by 34.6%. Fluxes at the side irradiation position are given in Fig. 8. It also shows that the maximum impact of density change are for the thermal flux. It will decreased by 15.3% with increasing the density from 3.2 to 6 g/cm³, and by 27.4% with increasing the density to 15 g/cm³. While for the other groups there is no clear impact.

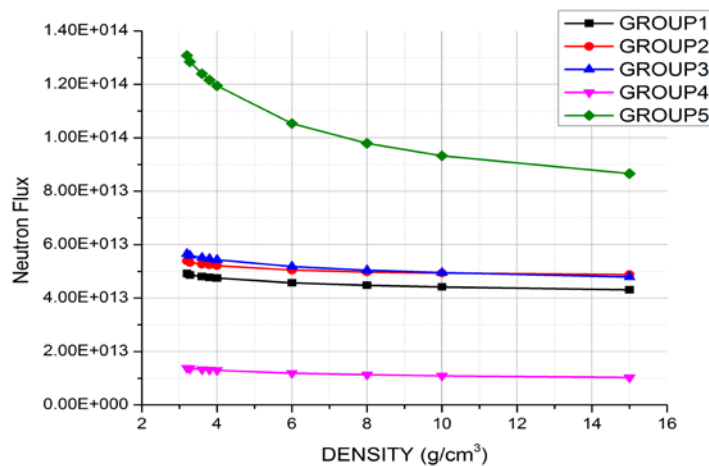


Figure 7: Neutron fluxes in the central irradiation position.

The plot of fluxes in the central irradiation position as a function of density change are shown in Fig. 7. As can be seen from the figure the thermal neutrons flux has the maximum impact of density change. By increasing the density from 3.2 to 6 g/cm³ the thermal neutron decreased by 19.2%, while by increasing the density to 15 g/cm³ the thermal flux decreased by 34.6%. Fluxes at the side irradiation position are given in Fig. 8. It also shows that the maximum impact of density change are for the thermal flux. It will decreased by 15.3% with increasing the density from 3.2 to 6 g/cm³, and by 27.4% with increasing the density to 15 g/cm³. While for the other groups there is no clear impact.

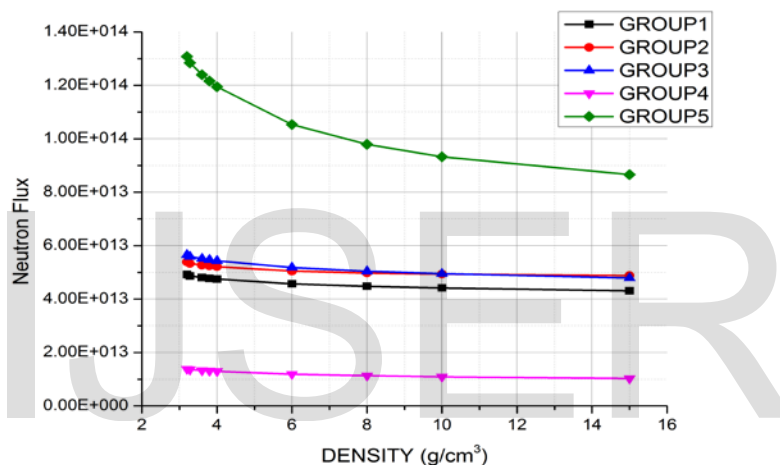


Figure 7: Neutron fluxes in the central irradiation position.

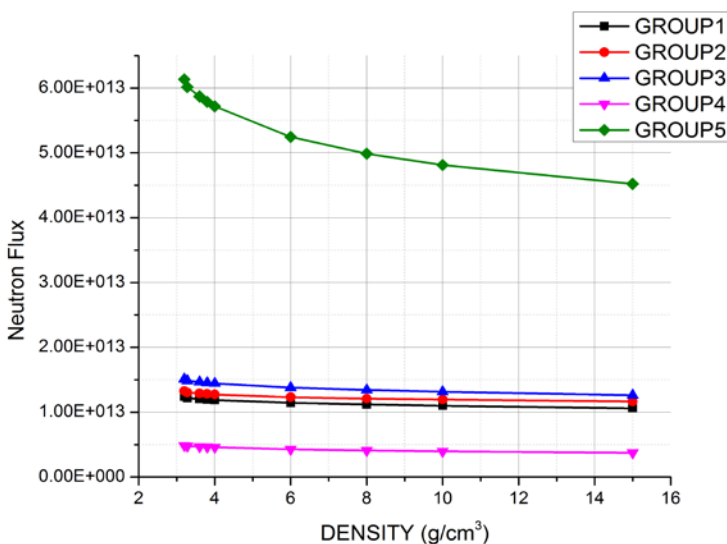


Figure 8: Neutron fluxes in the side irradiation position.

4.2 Equilibrium Cycle for the selected densities:

Equilibrium cycle: According to the different cycle length calculated for the selected densities the equilibrium cycle founded at cycle number 6 with length of 40 days for density 3.2 g/cm^3 , 46 days for density 3.8 g/cm^3 and 48 days for density 4 g/cm^3 . Thus, for density 3.2 g/cm^3 equilibrium cycle will begin at the day 200 and end at 240th day, for density 3.8 g/cm^3 the equilibrium cycle will begin at 230 and end at 276 and for density 4 g/cm^3 the equilibrium cycle will begin at the day 240 and end at 288th day.

The maximum and average burnup: The evaluation of the fuel burnup shows that; at the end of equilibrium cycle, the maximum burnup value for the standard fuel element was located at position C8 for all selected densities. It has the values of 52300, 52000 and 51600 MWD/Te for the densities 3.2, 3.8 and 4 g/cm^3 respectively. The average core burnup were 27546 MWD/Te for density 3.28 g/cm^3 , 27320 MWD/Te for density 3.8 g/cm^3 and 27073 MWD/Te for density 4 g/cm^3 . Thus, the resulting fuel burnup should not exceed the proved limit.

Excess reactivity control: In terms of reactivity control, the five control rods used within the selected core design has an average total 12810 pcm, which mean that; in case of using fuels with the density 3.28 g/cm^3 the control system will give us a shutdown margin with amount of 4815 pcm. In case of fuel density 3.8 g/cm^3 , it gives 2850 pcm as a shutdown margin. While it gives 2234 pcm as a shutdown margin for fuel with density 4 g/cm^3 . This means that the excess reactivity in all cases of fuel density is manageable with the control system.

5. Conclusions:

A neutronic analysis was performed for cores using fuel elements densities 3.2, 3.28, 3.6, 3.8, 4, 6, 8, 10 and 15 g/cm^3 to determine the impact on reactivity, multiplication factor, neutron flux, power density and burnup distribution. The impact of fuel density change on core reactivity was found to be

clear up to 6 g/cm³. For densities above 6 g/cm³, modifications of the core configuration are needed to enhance the reactivity. The change in k_{eff} through one cycle depends on the density change. For each fuel density used there is an optimum cycle length. The increase in the uranium density in the fuel elements caused the neutron flux in the irradiation positions to decrease. The central irradiation position the thermal neutron flux decreased by 19.2% with the density increase from 3.2 to 6 g/cm³. While increasing the density to 15 g/cm³ caused the thermal flux to decrease by 34.6%.

This means that we need to modify the increase the reflection of the core or to increase the power of the core to raise the neutron fluxes. The burnup distribution decreased with increasing fuel density in all fuel elements which extended the cycle length. The impact of increasing fuel density on the power density distribution was greater in fuel elements near the central irradiation position, due to the relatively high thermalization caused by the water inside the central flux trap. While it decreased in all other fuel elements. To implement this study in finding an optimum design of core configuration with high fuel density we propose to:

1. Test the optimum cycle length suggested for each density
2. Determine the optimum core volume
3. Determine the best reflector configuration
4. Find the optimum fuel shuffling to reach the equilibrium core

References:

- [1] IAEA-TECDOC-233 (1980). *Research Reactor Core Conversion from the Use of Highly Enriched Uranium to the Use of Low Enriched Uranium Fuels, Guidebook*. International Atomic Energy Agency (IAEA), Austria.
- [2] IAEA-TECDOC-643 (1992). *Research Reactor Core Conversion, guidebook*. Volume 1: Summary, International Atomic Energy Agency (IAEA), Austria.
- [3] Ahmed, R., Aslam, & Ahmad, N. (2005). Burnup study for Pakistan research reactor-1 utilizing high density low enriched uranium fuel. *Annals of Nuclear Energy*, 32: 1100-1121.
- [4] Muhammad, F., & Majid, A. (2009). Effects of high density dispersion fuel loading on the dynamics of a low enriched uranium fueled material test research reactor. *Progress in Nuclear Energy*, 51(2): 339–346.
- [5] Raina, V. K., Sasidharan, K., Sengupta, S., & Singh, T. (2006). Multi purpose research reactor. *Nuclear Engineering and Design*, 236: 770–783.
- [6] Muhammad, F. (2013). Effects of high density dispersion fuel loading on the control rod worth of a low enriched uranium fueled material test research reactor. *Annals of Nuclear Energy*, 58: 19–24.
- [7] Ahmad, S. I., Ahmad, N., & Aslam (2004). Effect of new cross-section evaluations on criticality and neutron energy spectrum of a typical material test research reactor. *Annals of Nuclear Energy*, 31: 1867–1881.
- [8] Ali Khan, L., Ahmad, N., Zafar, M. ., & Ahmad, A. (2000). Reactor physics calculations and their experimental validation for conversion and upgrading of a typical swimming pool type research reactor. *Annals of Nuclear Energy*, 27(10): 873–885.

- [9] Aslam, & Ahmad, N. (2002). Effect of coolant channel width on group constants and multiplication factor of research reactors using MTR type low enriched uranium fuel. *Annals of Nuclear Energy*, 29(4): 477–488.
- [10] Malkawi, S. R., & Ahmad, N. (2001). Solution of the neutron spectrum adjustment problem in a typical MTR type research reactor. *Annals of Nuclear Energy*, 28(1): 25–51.
- [11] Ahmad, S.-I., Ahmad, N., & Aslam (2006). Effect of different cross-section data sets on reflectors of a typical material test research reactor. *Progress in Nuclear Energy*, 48(2): 155–164.
- [12] Roth, M. J., Macdougall, J. D., & Kemshell, P. B. (1991). *WIMS-D user manual*.
- [13] Villarino, E. A., & Lecot, C. A. (1995). *CITVAP V3.1, a reactor calculation code, Nuclear Engineering Division, INVAP SE*. San Carlos de Bariloche, Argentina.
- [14] Fowler, T. B., Vondy, D. R., & Cunningham, G. W. (1999). CITATION--Nuclear Reactor Core Analysis Code. *ORNL_TM-2496*.
- [15] Pevey, R. E. (2009). Neutronics. In K. D. Kok (Ed.), *Nuclear Engineering Handbook*. CRC press Taylor & Francis, (pp. 575–608).
- [16] Ahmad, S.-I., & Ahmad, N. (2006a). Burnup-dependent core neutronics analysis and calculation of actinide and fission product inventories in discharged fuel of a material test research reactor. *Progress in Nuclear Energy*, 48(6): 599–616.